Hydraulic properties of adsorbed water films in unsaturated porous media

Tetsu K. Tokunaga

Earth Sciences Division, Lawrence Berkeley National Laboratory

Berkeley, California, USA

Abstract. Adsorbed water films strongly influence residual water saturations and hydraulic conductivities in porous media at low saturations. Hydraulic properties of adsorbed water films in unsaturated porous media were investigated through combining Langmuir's film model with scaling analysis, without use of any adjustable parameters. Diffuse double layer influences are predicted to be important through the strong dependence of adsorbed water film thickness (f) on matric potential (ψ) and ion charge (z). Film thickness, film velocity, and unsaturated hydraulic conductivity are predicted to vary with z^{-1}, z^{-2}, and z^{-3}, respectively. In monodisperse granular media, the characteristic grain size (λ) controls film hydraulics through λ^{-1} scaling of (1) the perimeter length per unit cross sectional area over which films occur, (2) the critical matric potential (ψ_c) below which films control flow, and (3) the magnitude of the unsaturated hydraulic conductivity when $\psi < \psi_c$. While it is recognized that finer textured sediments have higher unsaturated hydraulic conductivities than coarser sands at intermediate ψ, the λ^{-1} scaling of hydraulic conductivity predicted here extends this understanding to very low saturations where all pores are drained. Extremely low unsaturated hydraulic conductivities are predicted under adsorbed film-controlled conditions (generally < 0.1 mm y^{-1}). On flat surfaces, the film hydraulic diffusivity is shown to be constant (invariant with respect to ψ).

1. Introduction

Properties of adsorbed aqueous films determine conditions for residual water saturation in porous and fractured geologic media, and influence the dynamics of pore scale water displacement that determine macroscale distributions of immiscible fluids in the subsurface. Distribution of water relative to other immiscible fluids is of interest in hydrogeology, subsurface waste isolation using capillary barriers, petroleum engineering, and geologic carbon sequestration up to distances in excess of 10 km [e.g. *McPherson et al*., 2000; National Research Council, 2001]. Problems central to soil physics and irrigation agriculture span a broad range of scales from ≈ 10 m down to about 10^{-9} m [*Hillel*, 2004]. Thus, hydraulic properties of thin (nm to μm) films affect multiphase fluid flow and chemical transport in geologic formations over many orders of magnitude in length scale. Although moisture characteristics (saturation dependence on matric potential) and unsaturated hydraulic conductivity relations at low water contents are critical in all of the previously mentioned processes, they remain poorly understood. The complex geometry of pore networks and the strong influence that pore size exerts on water retention and viscous flow make it difficult to accurately predict moisture characteristics and unsaturated hydraulic conductivity relations without use of some empirical, adjustable parameters. The challenge of accurately representing moisture characteristics and unsaturated hydraulic conductivities of porous media has been addressed in many studies [e.g., *Mualem*, 1974; *van Genuchten*, 1980; *Luckner et al.,* 1989; *Durner*, 1994; *Assouline*, 2005; *Wei and Dewoolkar*, 2006].

Understanding the pore scale distribution of water in granular media and its impact on transport processes remains an outstanding challenge, especially at low saturations where films restrict flow. Indeed, processes occurring at low saturations are excluded in commonly

employed modeling approaches that rely on experimentally defined parameters "residual saturation" and "irreducible saturation". In recent years, some progress has been made on understanding water films retained on fracture and grain surfaces. The hydraulic properties of moderately thick films on rough surfaces, conceptualized as networks of surface capillary channels interspersed with thin films, have been measured and modeled [e.g. *Tokunaga and Wan*, 1997; *Blunt*, 1998; *Or and Tuller,* 1999; *Tokunaga et al*., 2001; *Tuller and Or*, 2002]. At near-zero matric potentials, capillary filling of depressions on rough surfaces results in thick water films that can support very high flow rates when sufficiently interconnected. Such high film fluxes on complex topography are relatively easily measured, and have been identified as an important mechanism for fast flow through the unsaturated zone. At lower matric potentials, capillary-filled grain surface channels become discontinuous, and much thinner adsorbed films control hydraulic behavior. While it is understood that unsaturated flow and transport are severely restricted by the hydraulic resistance of adsorbed thin films, the hydraulic properties of adsorbed films remain to be quantified. The extreme hydraulic resistance of thin films permit only minute fluxes, making measurements of their transmissivities (flow per unit transverse length, under unit hydraulic head gradient) very challenging. Moreover, interfacial physicochemical influences on film properties are complex and incompletely understood [e.g., *Muller*, 1998; *Goertz et al*., 2007]. Under these challenging conditions, it is still possible to gain understanding on film hydrostatics and hydrodynamics in model porous media through deducing implications of current knowledge. The present effort builds on analyses of scaling and interfacial physical chemistry in order to predict hydraulic phenomena at low saturations without use of any adjustable parameters.

Scaling methods are useful for predicting equilibrium and transport properties of porous media. *Miller and Miller* [1955a, 1956] developed the foundation for geometric capillary scaling of unsaturated hydraulic properties. The approach taken in Miller-Miller scaling generalizes physical/mechanical influences of length (grain or pore size), surface tension, and viscosity on virtual, geometrically similar porous media. Moisture retention and unsaturated hydraulic conductivity measurements on packs of glass beads and sands have demonstrated the validity of Miller-Miller similitude over a moderate range of length scales (grain sizes from 0.05 to 1.1 mm) and levels of water saturation down to about 15%. It is important to note that the range of applicability of Miller-Miller scaling is restricted to conditions where capillary forces control the pore scale distribution of the wetting liquid in geometrically similar media. Within these limits, predicted relations between saturation, matric (capillary) potential, and unsaturated hydraulic conductivity have been shown to be reliable [*Miller and Miller*, 1955b; *Klute and Wilkinson*, 1958; *Schroth et al.,* 1996]. A number of generalized approaches to scaling of porous media hydraulic properties have since been developed that have fewer restrictions [e.g., *Hillel and Elrick*, 1990; *Snyder*, 1996]. All of these studies have helped build a unified framework through which to predict unsaturated hydrostatic and hydrodynamic behavior.

Scaling analyses are also useful for understanding limitations on familiar hydraulic behavior. Departure from continuum behavior describable by Richards equation was recently identified by *Or* [2008] at a Bond number $(\Delta\rho g R^2/\sigma)$ of about 0.05, where $\Delta\rho$ is the mass density difference between immiscible fluids, g is the acceleration of gravity, R is the characteristic pore radius, and σ is the fluid-fluid interfacial tension. At a still larger Bond number of about 0.5, gravity (more generally, body forces) dominates over capillarity and leads to the disappearance of capillary hysteresis in monodisperse granular media with grain sizes greater than 10 mm

[*Tokunaga et al.,* 2004]. Based on direct tests of the Kelvin equation, *Fisher and Israelachvili* [1979] showed that capillary curvature-potential relations extend down to at least 4 nm. Thus, capillary scaling can predict aspects of granular media hydraulics over at least 5 orders of magnitude in grain size (10^{-7} to 10^{-2} m). However, within this very broad range of grain sizes exists a poorly understood region of hydraulic behavior in porous media associated with saturations low enough that water retained in pendular rings no longer form directly interconnected networks. Below a critical matric potential, ψ_c, thin films of adsorbed water mediate fluxes between adjacent pendular rings (Figure 1). Because adsorbed water films are much thinner than dimensions of capillary/pendular rings, practically all the hydraulic resistance resides within the films during unsaturated flow at very low saturation. Capillary scaling can be used to identify the scale dependence of ψ_c, but surface physicochemical relations will also be needed to understand adsorbed film properties.

Although water retention at low saturations in soils with polydisperse grain size distributions and idealized model systems has been investigated [e.g., *Rossi and Nimmo*, 1994; *Davis et al*., 1990; *Toledo et al.,* 1990; *Blunt*, 1998; *Or and Tuller*, 1999; *Tuller and Or*, 2002; *Silva and Grifoll*, 2007], it is difficult to clearly isolate effects of adsorbed films in complex systems. The unsaturated hydraulic conductivity at intermediate saturations is largely determined by networks of interconnected pendular rings, often idealized as networks of interconnected capillary corners following *Ransohoff and Radke* [1988]. Few studies have focused on isolating the nature of adsorbed films in porous media that ultimately limit flow and transport when capillary connections between pendular rings and surface channels become discontinuous. *Waldron et al.* [1961] employed several methods to establishing hydrostatic equilibrium by drainage of initially saturated monodisperse media, and obtained results

indicating that significantly more water is retained than predicted from retention in pendular rings. Investigating a lower range of water potentials and approaching equilibrium via wetting (vapor adsorption), *Jurinak et al.* [1962] obtained results indicative of much thinner films in their study on monodisperse glass spheres. To date, no studies appear to have compared such results with model predictions, or addressed film hydraulics in the context of its scale dependence. In order to achieve these goals, a conceptual framework is needed for relating film thicknesses to grain size and matric potential. Such an understanding will also resolve a basic uncertainty concerning flow at very low saturations. Will films on higher surface areas associated with finer granular media support higher flow rates at low saturation relative to coarser granular media? Although it is well known that clays are more hydraulically conductive than sands at intermediate matric potentials because of greater continuity of capillary-filled pores, similar understanding is lacking for conditions where films control flow. In addition to flow, basic understanding of transport and biogeochemical processes in variably saturated soils and sediments requires information on film thicknesses. For example, the mobility of colloids through unsaturated soils is strongly restricted by thin films [*Wan and Tokunaga*, 1997; *Gao et al.,* 2006]. The rapidly developing activities in geologic CO_2 sequestration present an important new set of environmental conditions where understanding aqueous films will be important because they will mediate reactions between CO_2 and mineral surfaces, and provide an immiscible boundary layer for CO_2 invading pores [*Suekane et al*., 2005].

The aforementioned issues highlight the importance of understanding thin films in porous media. This study presents calculations of thin water film hydrostatics and hydrodynamics under conditions of low ionic strength solutions, with film viscosities equal to those of bulk water. Through these calculations, the scale dependence of thin film hydraulics is shown to arise from

geometric, capillary, and interfacial effects. These results are then used to estimate bulk unsaturated hydraulic conductivities of granular porous media at low saturations.

2. Model Development

At low water saturations in monodisperse, hydrophilic granular media, flow is controlled by thin films coating grain surfaces. The microscopic scale of the granular/porous medium can be defined by the grain diameter λ, which will be shown to influence film hydraulic phenomena in several ways. One major influence is on the abundance of films, and is strictly geometric. From dimensional considerations of geometrically similar porous media, both the specific surface (surface area per unit volume), and specific perimeter (P_s, grain perimeter length per unit cross-section area) scale as λ^{-1}. Therefore, at low water saturations, thin film flow is localized on grain perimeters, which per unit bulk area increases as grain size decreases. A functional relation between P_s and λ can be obtained for monodisperse packs of spherical grains by first determining the number of grains N_o intercepting a plane of unit area A_o in a porous medium. Such a plane will intercept grains with centroids located within a distance of $\lambda/2$ on either side of it. Therefore, grains centered within a reference bulk volume of unit cross-section area A_o and thickness λ will have perimeters that project onto the unit cross-section surface. With a porosity n, the solid phase volumetric fraction of $1 - n$ is equal to the ratio of the solid volume per unit bulk volume. For the reference volume of $A_o\lambda$,

$$1 - n = \frac{N_0 \pi \lambda^3}{6 A_0 \lambda} \tag{1}$$

where N_o is the number of spheres centered within the bulk volume, each with a volume of $\pi\lambda^3/6$. Therefore, the number of grains intercepting a unit cross-section area is

$$\frac{N_0}{A_0} = \frac{6(1-n)}{\pi\lambda^2} \tag{2}$$

For interceptions of grains with a reference plane, any given grain projects a perimeter equal to $\pi\lambda sin\phi$, where ϕ is the polar angle associated with the sphere-plane intersection (sphere axis normal to the plane). Thus, the average intercepted perimeter per grain is

$$\overline{P_i} = \lambda \int_0^{\pi} \sin\phi d\phi = 2\lambda \tag{3}$$

The specific perimeter P_s is simply the product of equations (2) and (3)

$$P_s = \frac{12}{\pi\lambda}(1-n) \tag{4}$$

showing how P_s scales inversely with λ and linearly with the solid volume fraction *(1-n)*. Approaches to analyzing perimeters in more complex systems are available in the stereology literature [Baddeley and Vedel Jensen, 2005]. This expression by itself suggests that thin film flow could be more effective upon desaturation of finer granular media than coarser granular media. However, film thicknesses and thin film transmissivities are themselves potential-dependent. Before developing these relations, it is important to determine the scale dependence of the film-limited range of matric potentials.

In order to reach hydraulic conditions where thin films control viscous flow, the matric potential must be lower (more negative) in finer granular media in order to overcome capillary filling of pores. In his classic paper on hysteresis of moisture characteristics, *Haines* [1930] showed that main drainage in a monodisperse close packing of spherical grains occurs at a capillary (matric) potential of $\psi_d \approx -26\sigma/\lambda$, and that saturation of main pore bodies occurs at an unspecified potential of much smaller magnitude. Thus, a second significant influence of λ on films occurs through determining the threshold ψ below which thin films control flow and transport through the aqueous phase. The energy at which pendular rings become reconnected is

at an intermediate value relative to ψ_d. In close packing of perfectly water-wet (zero contact angle), monodispersed spherical grains, the critical potential at which pendular rings connect and disconnect is illustrated in Figure 2.

Under these conditions, the critical matric potential is

$$\psi_c \approx -9.1\frac{\sigma}{\lambda} \tag{5}$$

[*Fisher*, 1926; *Haines*, 1930; *Melrose and Wallick*, 1967]. *Fisher* [1926] derived equations for pendular ring geometries, and showed that the water saturation due to pendular rings is 24.3% at the critical condition for close packed spheres. *Haines* [1930] showed that pendular ring connection/disconnection at $\psi = \psi_c$ only occurs along the main wetting curve, that pore bodies remain water-filled when ψ_c is approached from saturation, and that equilibrium drainage to $\psi_d \approx -26\sigma/\lambda$ must be reached via conduction through adsorbed films (Figure 3). Given the very low hydraulic conductivities of thin films between pendular rings (estimated later), true desaturation equilibrium within any macroscopic volume of porous medium can only be reached after long drainage times.

Understanding how film thickness depends on potential is most important at energies below $\psi_c \approx -9.1\sigma/\lambda$ during saturation, and below $\psi_d \approx -26\sigma/\lambda$ during drainage because these are the conditions under which thin films control flow. Relations between the Gibbs free energy of aqueous films and film thickness have been examined in numerous investigations [e.g., *Langmuir*, 1938; *Read and Kitchener*, 1969; *Derjaguin et al.,* 1987; *Israelachvili*, 1991]. *Langmuir* [1938] derived an expression for the film thickness, f, by equating the counterion distribution within adsorbed films with that occurring in a solution bounded by parallel solid surfaces separated by a distance of $2f$. Assuming the electrostatic potential profile within the half space between parallel solid surfaces and their midplane are equivalent to that within adsorbed

water films bounded by a single solid surface and the air-water interface, *Langmuir* [1938] solved the Poisson-Boltzmann equation for the case of large electrostatic potentials within the film and no gradient in the potential at the water-air interface, obtaining

$$f = \sqrt{\frac{\varepsilon\varepsilon_0}{2}}\left(\frac{\pi k_B T}{ze}\right)(-\psi)^{-0.5} \tag{6}$$

where ε is the relative permittivity of water (78.54), ε_o is the permittivity of free space (8.85 x 10^{-12} C^2 J^{-1} m^{-1}), k_B is the Boltzmann constant (1.381x10^{-23} J K^{-1}), T is the Kelvin temperature, z is the ion change, and e is the electron charge (1.602x10^{-19} C). It should be noted that equation (6) was obtained through assuming electrostatic potentials are large throughout the film, and much higher than k_bT at the solid-water interface. From the Grahame equation [*Israelachvili*, 1991], these conditions are predicted to be satisfied approximately in dilute aqueous solutions. As noted previously, equating an adsorbed water film to a single half-space between two solid surfaces also introduces the assumption of a strictly neutral air-water interface, in which the electrostatic potential gradient vanishes. This continuum assumption fails at the nm scale of strong molecular interactions because of water molecule structure and orientation at the air-water interface [e.g., *Muller*, 1998; *Beattie et al.,* 2009]. Although Langmuir's original derivation was applied to study fairly thick adsorbed films above capillary menisci, it has since been tested over wider ranges of conditions. *Read and Kitchener* [1969] found that the Langmuir equation provided fairly good estimates of the valence dependence of thicknesses of dilute aqueous films adsorbed on hydrophilic, moderately charged, flat silica surfaces. Experimental results from six different studies (including that of *Read and Kitchener*, 1969) supporting predictions of the Langmuir equation were summarized in *Derjaguin and Churaev* [1974]. It should be noted that equation (6) is not expected to apply well to films thinner than several nm because, as an electrostatic continuum model, it does not account for molecular scale interactions at either

water-solid or water-air interfaces. We show later that such extremely thin adsorbed water films (as opposed to water confined in nanopores) can only occur at very low matric potentials (< -10^5 Pa). Note that there are no adjustable parameters contained in equation (6), including the Hamaker constant which has a wide range of reported values associated with water-oxide systems [*Ackler et al.,* 1996]. Thus, equation (6) will be used as a working hypothesis for predicting film behavior in model porous media, to be tested and improved upon as more direct measurements become available. On smooth hydrophilic grain surfaces, an additional component of pressure results from surface tension of the convex adsorbed film, which increases in magnitude for smaller grains because of their higher curvature. *Wan and Tokunaga* [1997] modified Langmuir's result to account for these surface tension and curvature effects through

$$f = \sqrt{\frac{\varepsilon\varepsilon_0}{2}}\left(\frac{\pi k_B T}{ze}\right)\left(\frac{2\sigma}{\lambda} - \psi\right)^{-0.5} \tag{7}$$

Thus, another influence of the microscopic scale λ is on thicknesses of adsorbed films. We show later that this grain size effect is relatively minor compared to that of the matric potential. In monodisperse, close packed media, equation (7) applies only in drained pores, with $\psi < \psi_c$. Substituting equation (5) into equation (7) gives $f(\lambda, \psi_c)$ for ψ implicitly at critical values ψ_c associated with continuously variable λ, as

$$f_c(\lambda) \approx \sqrt{\frac{\varepsilon\varepsilon_0}{22}}\left(\frac{\pi k_B T}{ze}\right)\sqrt{\frac{\lambda}{\sigma}} \tag{8a}$$

and the film thickness at ψ_c as

$$f_c(\psi_c) \approx \sqrt{\frac{\varepsilon\varepsilon_0}{22}}\left(\frac{3\pi k_B T}{ze}\right)\psi_c^{-0.5} \tag{8b}$$

The final influence of scale on film phenomena considered in this analysis is on flow. The average film velocity under a unit potential gradient can be approximated by integration of a parabolic dependence on f with zero slip at the interface with the solid surface [*Bird et al.,* 1960]

$$\bar{v} = \frac{\rho g}{3\eta} f^2 \tag{9a}$$

where ρ and η are the fluid density and viscosity, respective. Substituting equation (7) into (9a) gives an estimated average film velocity at ψ, under unit hydraulic head gradient,

$$\bar{v}(\lambda,\psi) \approx \frac{\rho g \varepsilon \varepsilon_0}{6\eta}\left(\frac{\pi k_B T}{ze}\right)^2 \frac{\lambda}{2\sigma - \lambda\psi} \tag{9b}$$

Note that equation (9b) is not applicable for $\psi > \psi_c$ because pendular rings become interconnected and pores water-saturated under this condition. The apparent scale-dependence of equation (9b) will be discussed later. Substituting equation (8) into (9a) gives the estimated average film velocity at ψ_c, under unit hydraulic head gradient,

$$\bar{v}(\lambda,\psi_C) \approx \frac{\rho g \varepsilon \varepsilon_0}{66\eta}\left(\frac{\pi k_B T}{ze}\right)^2 \frac{\lambda}{\sigma} \tag{9c}$$

Both equations (9b) and (9c) are approximate because flow at $\psi < \psi_c$ does not occur in simple unidirectional vertical films at the grain scale. Rather, grain-scale film flow involves more complex streamline networks that converge and diverge at gradient-selected, nearest neighbor pendular rings. In addition, the above relations will significantly overestimate velocities in films thinner than about 10 nm, as discussed later.

The flux per unit perimeter length under unit hydraulic gradient is estimated by multiplying the thickness-averaged velocity by f

$$\bar{v} f = \frac{\rho g}{3\eta} f^3 \tag{10}$$

In the case of downward flow of and adsorbed film on a vertical planar surface, this flux per unit horizontal length has been termed the film transmissivity, T [*Tokunaga and Wan,* 1997]. In monodisperse close packing, the approximate film flux per bulk cross section of porous medium under a unit hydraulic head gradient is given by the product of equations (4) and (10), resulting in

$$Q_1 \approx \frac{4\rho g}{\pi\eta}\frac{(1-n)}{\lambda} f^3 \tag{11}$$

Incorporating the potential- and scale-dependence of f gives the estimated unsaturated hydraulic conductivity below ψ_c as

$$K(\psi \le \psi_c, \lambda) \approx \frac{4\pi^2\rho g(1-n)}{\eta\lambda}\left(\frac{\varepsilon\varepsilon_0}{2}\right)^{1.5}\left(\frac{k_B T}{ze}\right)^3\left(\frac{2\sigma}{\lambda}-\psi\right)^{-1.5} \tag{12a}$$

and at ψ_c as

$$K(\psi_c, \lambda) \approx \frac{4\pi^2\rho g}{\eta}\left(\frac{\varepsilon\varepsilon_0}{22\sigma}\right)^{1.5}\left(\frac{k_B T}{ze}\right)^3 (1-n)\sqrt{\lambda} \tag{12b}$$

3. Results and Discussion

Example curves for the predicted dependence of film thickness on grain scale and matric potential, $f(\lambda, \psi)$, are shown for several values of λ in Figure 4. These curves were obtained from equation (7), for dilute monovalent aqueous solutions. The Langmuir-predicted thicknesses for dilute divalent aqueous solutions are simply half the values shown in Figure 4. Thus, over the matric potential range encountered in most of the subsurface, film thicknesses are predicted to range from a few nm up to about 200 nm when pore sizes are large enough to prevent capillary pore filling. The calculated film thicknesses shown in Figure 4 are also expressed in terms of numbers of molecular layers of water along the right vertical axis. For this purpose, the

monolayer thickness of 0.311 nm was used, based on the cube-root of the liquid water molecule specific volume at 20 ˚C. The effects of film curvature and surface tension are evident in the progressively thinner films with smaller grain sizes shown in this figure. Values of ψ_c given by equations (8a) and (8b) are indicated on the example curves for specific λ values by open circles in Figure 4. Below ψ_c, viscous flow is controlled by films through P_s varying with λ^{-1} (equation (4)), with scale dependence of film thickness being approximately $\lambda^{0.5}$ (equations (7) and (8a)). Note that $-\psi_c$ is large relative to $2\sigma/\lambda$, so that differentiation of equation (7) gives $df/d\psi \approx -f/(2\psi)$. Thus, film thickness changes approximately hyperbolically with respect to matric potential. The magnitude of ψ_c relative to $2\sigma/\lambda$, also shows that the matric potential dominates over surface tension in controlling film thickness, regardless of grain-size.

Contributions of adsorbed films to model porous media saturations can now be calculated through combining the Langmuir-based results with Fisher's pendular ring volumes. The geometry of monodisperse spherical grains in close packing permits such calculations in a simple manner. Below ψ_c, each grain is surrounded by 12 pendular rings. Because each pendular ring bridges 2 grains, each grain is associated with volumetric water contributions from 6 complete rings. The matric potential dependent pendular ring footprints (pendular ring contact areas on spheres), and saturations due to pendular rings were obtained for different grain sizes using results from *Fisher* [1926, Table 1]. These capillary contributions to saturations are shown as dashed curves in Figure 5, for 4 different grain sizes. Each curve terminates at a maximum at $S_c(\psi_c)$ indicated by an open circle. The similarity between these dashed curves (identical shapes, offset along the potential axis) reflects λ^{-1} capillary scaling. The volumetric contribution of adsorbed films was calculated using equation (7), applied to fractions of surfaces not covered by 12 pendular rings per grain. The matric potential-dependent total (pendular ring and adsorbed

film) saturations for 4 grain sizes are shown as solid lines in Figure 5. The volumetric contributions of water films to the saturation are represented by the increased saturation obtained by moving vertically from the dashed curves to the solid curves. These plots show relatively small saturation contributions from films, except when the matric potentials are much lower (more negative) than ψ_c and when grain size is small. Comparisons with water drainage data reported by *Waldron et al*. [1961] over a range of matric potentials, and water vapor adsorption data reported by *Jurinak et al.* [1962] at their highest vapor pressures ($P/P_o = 0.980$, equivalent to a matric potential of -2.7 MPa) are also shown in Figure 5. The estimated film thickness from *Jurinak et al.* [1962] is about 3.0 molecular layers of water at this potential, and is in very good agreement with our model prediction of 2.9 molecular layers. *Collis-George and Bozeman* [1970] suggested that the higher saturations obtained by *Waldron et al*. [1961] reflect nonequilibrium drainage, and will be discussed later.

The dependence of average film velocity on matric potential, grain scale, and ion charge predicted using equation (9b,c) is summarized in Figure 6. Values for water parameters were taken as those of pure water at 293 K ($\rho = 998$ kg m^{-3}, $\eta = 1.00$ mPa s, $\sigma = 72.7$ mN m^{-1}). The grain scale-dependence of film velocity at ψ_c is shown through the upper v limit (open circles) increasing with λ. Note however, that when $\psi < \psi_c$, film velocities are relatively insensitive to grain size. This approximate scale invariance of film velocities at any given $\psi < \psi_c$, reflects the relatively minor grain scale influence on f under these drained conditions previously presented in Figure 4. The influence of solution chemistry occurs through the inverse square dependence on ion charge, and is expected to have a major impact. Thus adsorbed films containing monovalent ions are predicted to move 4 times faster than films containing divalent ions under the same hydraulic gradient. It is also important to note that these velocities are very low, in the range of

mm y^{-1} to m y^{-1}. Darcy (volumetric) fluxes are even lower because of the very low cross-sectional areas associated with thin films. The very low velocities presented in Figure 6 show that up to moderate distances and times, diffusion is much more efficient for transporting solutes in adsorbed films than advection.

A potentially greater uncertainty in predicted fluxes arises from the viscosity, for which wide ranges of departures from bulk values have been measured on film thicknesses less than a few nm (*Horn et al.,* 1989; *Raviv et al.,* 2001), supporting predictions of *Kemper* (1960, 1961). Inspection of Figure 4 indicates such departures from bulk water viscosities will be dominant at matric potentials less than about -10^5 Pa (-1 bar). The greater viscosity within a few nm of the solid surface also affects fluxes in thicker films because of the nonlinear, approximately parabolic velocity profile. Film thicknesses of about 10 to 20 nm may be required before average fluxes approach those consistent with the bulk water viscosity (*Kemper,* 1961). Thus, the predictions developed here are expected to be useful for estimating magnitudes of unsaturated hydraulic conductivities in drained coarse granular media down to about -10^4 Pa, but will significantly overestimate film fluxes regardless of grain size below this potential.

In order to estimate $K(\psi,\lambda)$ using equation (12a,b), ρ, η, and σ were taken as values for pure water at 293 K (20 ˚C). A porosity $n = 0.2595$ was used for this calculation on ideal close packing of monodisperse spheres. Estimated $K(\psi)$ dependence on λ and z are shown in Figure 7. These $K(\psi)$ are extremely low, corresponding to flux densities that are at most 0.1 mm y^{-1}, and decrease to well below nm y^{-1}. An important consequence of such low $K(\psi)$ is that very long times are required to attain true hydraulic equilibrium. For this reason, the higher saturations obtained in drainage of monodisperse spheres by *Waldron et al*. [1961] might have resulted from not reaching equilibrium [*Collis-George and Bozeman*, 1970]. Although these saturations were

higher than predicted equilibrium levels, they are all well below S_c. This indicates that pendular rings were discontinuous and that drainage was restricted by thin films. The expression for the unsaturated hydraulic conductivity at ψ_c, equation (12b), predicts that film flow in porous media increases with the square-root of grain size, reflecting the balance between the $\lambda^{1.5}$ scaling arising from the cubic dependence on film thickness, and the λ^{-1} scaling of specific perimeter through which film flow occurs. This may suggest that film flow decreases with λ because restrictions of thinner films dominate over their increased perimeter. However, this relation holds only at $\psi_c(\lambda)$, not at a specified ψ. It is clear from inspection of Figure 7 that at any common value of ψ where pendular rings are discontinuous, $K(\psi)$ increases with decreased grain size. Equation (12a) predicts that $K(\psi)$ scales approximately with λ^{-1} in the film-controlled region because it encompasses conditions where $\psi \leq 9\sigma/\lambda << 2\sigma/\lambda$. Thus, finer granular media are more hydraulically conductive than similar coarser media at any specified matric potential, even when pores are desaturated, and advection is controlled by adsorbed films. This scaling of $K(\psi)$ for adsorbed films results directly from the same λ^{-1} scaling of P_s.

Another important prediction of equations (12a,b) is that solutes have a strong impact on film flow of dilute solutions because of the inverse cubic dependence on ionic charge. Thus, solutions of monovalent ions support film fluxes that are 8 times greater than those of divalent ions. Recall that equation (12a,b) contains no adjustable parameters, but remains an approximation because a unit hydraulic gradient is assumed to apply along all grain surfaces at the film scale. As noted previously, film fluxes at ψ progressively lower than -10^4 Pa are expected to be progressively slower than the predictions based on bulk film viscosities.

The hydraulic properties of adsorbed films on flat surface can also be explored further in the limit of $\lambda \rightarrow \infty$. In this limit, substituting equations (7) and (9b) in (10) results in the

volumetric flux per unit wetted length under unit hydraulic head gradient, or the film transmissivity T.

$$\mathrm{T} = \frac{\rho g}{3\eta}\left(\frac{\varepsilon\varepsilon_0}{2}\right)^{1.5}\left(\frac{\pi k_B T}{ze}\right)^3 (-\psi)^{-1.5} \tag{13}$$

The adsorbed film hydraulic capacity on a flat surface is the change in film thickness per unit change in matric head, $h_m = \psi/(\rho g)$,

$$\frac{df}{dh_m} = \frac{\rho g}{2}\sqrt{\frac{\varepsilon\varepsilon_0}{2}}\left(\frac{\pi k_B T}{ze}\right)(-\psi)^{-1.5} \tag{14}$$

The film hydraulic diffusivity, D_f, is defined to be analogous to the bulk unsaturated hydraulic diffusivity [*Tokunaga et al.,* 2001], and is therefore obtained through dividing equation (13) by equation (14)

$$D_f = \frac{\varepsilon\varepsilon_0}{3\eta}\left(\frac{\pi k_B T}{ze}\right)^2 \tag{15}$$

This shows that the hydraulic diffusivity of adsorbed films on flat surfaces is constant, i.e. independent of ψ and f, because both T and df/dh_m vary as $-\psi^{-1.5}$. Using previously mentioned values of parameters, equation (15) predicts $D_f = 1.45 \times 10^{-9}$ and 3.63×10^{-10} m^2 s^{-1}, for $z = 1$ and 2, respectively. Practically constant D_f are expected to apply in the case of granular media well below ψ_c when saturations are dominated by contributions from adsorbed films rather than pendular rings. Thus, when a wetting film is controlled by double layer interactions according to Langmuir's model, its advance through simple media (flat surfaces and monodisperse packs of smooth grains) occurs with the film front broadening in an ordinary diffusive manner. Departures from constant hydraulic diffusivity involving lesser and greater spreading have been termed hypodispersive and hyperdispersive, respectively, and have been related to fractal properties of more complex natural porous media [*de Gennes*, 1985; *Davis et al*., 1990].

4. Summary

Both grain scale and solution ionic composition are predicted to be important in controlling unsaturated properties at low saturations, where adsorbed water films limit flow. This analysis of ideal granular media at low water saturation shows that grain scale influences film hydraulics through (1) the perimeter length per unit cross sectional area within which films occur, (2) the critical matric potential (ψ_c) below which films control flow, and (3) the magnitude of the unsaturated hydraulic conductivity when $\psi < \psi_c$. Each of these factors scale with the inverse of grain size. Therefore, finer granular media are predicted to have higher unsaturated hydraulic conductivities than coarser media, even when pores are fully drained. Because diffuse double layer thicknesses depend on counter-ion charge (z), solution chemistry is predicted to strongly influence adsorbed water film thicknesses. At low water contents, film thickness, film velocity, and unsaturated hydraulic conductivity are predicted to vary approximately with z^{-1}, z^{-2}, and z^{-3}, respectively. These strong solution chemistry-dependent influences only arise in the film-controlled limit.

Experimental testing of predictions developed in this study remain challenging because of extremely low fluxes and long equilibration times associated with adsorbed film flow. However, recent advances in nanotechnology, microfluidics, microtomography, and microscopy may soon permit direct measurements of adsorbed film hydraulics in porous media. Nanomachining can provide solid substrates with well-characterized topography on which experimental testing of capillary and adsorption effects can be conducted using solids with different surface properties in combination with different combinations of wetting fluids. Even with the availability of new methods and instruments, the very small mass transfer rates involved

in adsorbed film processes will require careful attention to controlling temperature disturbances and minimizing evaporative losses. As experiments tests of adsorbed film hydraulic properties become available, we will better understand the lower limits of unsaturated flow in porous media.

Acknowledgments. I thank the anonymous reviewers and Associate Editor John Selker for their careful review and helpful comments. Funding provided by the U.S. DOE, Office of Science, Basic Energy Sciences, Geosciences Research Program, under Contract No. DE-AC02-05CH11231, is gratefully acknowledged.

References

Ackler, H. D., R. H. French, and Y.-M. Chiang (1996), Comparisons of Hamaker constants for ceramic systems with intervening vacuum or water: From force laws and physical properties, *J. Colloid Interface Sci., 179*, 460-469.

Assouline, S. (2005), On the relations between pore size distribution index and characteristics of the soil hydraulic functions, *Water Resour. Res. 41*, W07019, doi:10.1029/2004WR003511.

Baddeley, A., and E. B. Vedel Jensen (2005), *Stereology for Statisticians*, 395 pp., Monographs on Statistics and Applied Probability 103, Chapman and Hall, CRC, Boca Raton, FL.

Beattie, J. K., A. M. Djerdjev, and G. G. Warr (2009), The surface of neat water is basic, *Faraday Discussions, 141*, 31-39.

Bird, R. B., W. E. Stewart, and E. N. Lightfoot (1960), *Transport Phenomenon*, 780 pp., Wiley, New York.

Blunt, M. (1998), Physically-based network modeling of multiphase flow in intermediate-wet porous media, *J. Petrol. Sci. Eng., 20*, 117-125.

Collis-George, N., and J. M. Bozeman (1970), A double layer theory for mixed ion systems as applied to the moisture content of clays under restraint, *Australian J. Soil Res., 8*, 239-258.

Davis, H. T., R. A. Novy, L. E. Scriven, and P. G. Toledo (1990), Fluid distribution and transport in porous media at low wetting phase saturations, *J. Phys. Condens. Matter, 2*, SA457-SA464.

de Gennes, P. G. (1985), Partial filling of fractal structure by a wetting fluid, in *Physics of Disordered Materials*, D. Adler, H. Fritzsche, and S. R. Ovshinsky, editors, 850 pp., Plenum, New York.

Derjaguin, B. V., and N. V. Churaev (1974), Structural component of disjoining pressure, *J. Colloid Interface Sci., 49*, 249-255.

Derjaguin, B. V., N. V. Churaev, and V. M. Muller (1987), *Surface Forces*, 440 pp., Consultants Bureau, New York.

Durner, W. (1994), Hydraulic conductivity estimation for soils with heterogeneous pore structure, *Water Resour. Res., 30*, 211-223.

Fisher, R. A. (1926), On the capillary forces in an ideal soil; Correction of formulae given by W. B. Haines, *J. Agric. Sci., 16*, 492-503.

Fisher, L. R., and J. N. Israelachvili (1979), Direct experimental verification of the Kelvin equation for capillary condensation, *Nature, 277*, 548-549.

Gao, B., J. E. Saiers, and J. Ryan (2006), Pore-scale mechanisms of colloid deposition and mobilization during steady and transient flow through unsaturated granular media, Water Resources Res., 42, W01410, doi:10.1029/2005WR004233.

Goertz, M. P., J. E. Houston, and X.-Y. Zhu (2007), Hydrophilicity and the viscosity of interfacial water. *Langmuir, 23*, 5491-5497.

Haines, W. B. (1930), Studies in the physical properties of soils, V. The hysteresis effect in capillary properties, and the modes of moisture distribution associated therewith, *J. Agric. Sci., 20*, 97-116.

Hillel, D. (2004), *Introduction to Environmental Soil Physics*, 494 pp., Academic, San Diego.

Hillel, D., and D. E. Elrick (1990), *Scaling in Soil Physics: Principles and Applications*, SSSAJ Special Publication Number 25, Soil Sci. Soc. Am., Madison, WI.

Horn, R. G., D. T. Smith, and W. Haller (1989), Surface forces and viscosity of water measured between silica sheets, *Chem. Phys. Lett. 162*, 404-408.

Israelachvili, J. N. (1991), *Intermolecular and Surface Forces, 2nd Edition*, 450 pp., Academic, London.

Jurinak, J. J., L. J. Waldron, and J. A. Vomocil (1962), Evidence of polymolecular film formation during adsorption of water and ethylene dibromide on glass spheres, *Soil Sci. Soc. Am. Proc., 26*, 433-436.

Kemper, W. D. (1960), Water and ion movement in thin films as influenced by the electrostatic charge and diffuse layer of cations associated with clay mineral surfaces, *Soil Sci. Soc. Am. Proc., 24*, 10-16.

Kemper, W. D. (1961), Movement of water as effected by free energy and pressure gradients: I. Application of classic equations for viscous and diffusive movements to the liquid phase in finely porous media, *Soil Sci. Soc. Am. Proc., 25*, 255-250.

Klute, A., and G. E. Wilkinson (1958), Some tests of the similar media concept of capillary flow: 1. Reduced capillary conductivity and moisture characteristic data, *Soil Sci. Soc. Am. Proc., 22*, 278-281.

Langmuir, I. (1938), Repulsive forces between charged surfaces in water, and the cause of the Jones-Ray effect, *Science, 88*, 430-432.

Luckner, L., M. Th. Van Genuchten, and D. R. Nielsen (1989), A consistent set of parametric models for the two-phase flow of immiscible fluids in the subsurface, *Water Resour. Res., 25*, 2187-2193.

McPherson, B. J. O. L., and B. S. Cole (2000), Multiphase CO_2 flow, transport and sequestration in the Powder River Basin, Wyoming, USA, *J. Geochemical Exploration 67-70*, 65-69.

Melrose, J. C., and G. C. Wallick (1967), Exact geometric parameters for pendular ring fluid, *J. Phys. Chem. 71*, 3676-3678.

Miller, E. E., and R. D. Miller (1955a), Theory of capillary flow: I. Practical implications, *Soil Science Soc. Am. Proc., 19*, 267-271.

Miller, E. E., and R. D. Miller (1955b), Theory of capillary flow: II. Experimental information, *Soil Sci. Soc. Am. Proc., 19*, 271-275.

Miller, E. E., and R. D. Miller (1956), Physical theory for capillary flow phenomena, *J. Appl. Phys., 27,* 324-332.

Mualem, Y. (1974), A conceptual model of hysteresis, *Water Resour. Res., 10*, 514-520.

Muller, H. J. (1998), Extraordinarily thick water films on hydrophilic solids: A result of hydrophobic repulsion?, *Langmuir, 14*, 6789-6792.

National Research Council (2001), *Conceptual Models of Flow and Transport in the Fractured Vadose Zone*, 374 pp., National Academy Press, Washington, D.C.

Or, D. (2008), Scaling of capillarity, gravity and viscous forces affecting flow morphology in unsaturated porous media, *Adv. Water Resour., 31*, 1129-1136.

Or, D., and M. Tuller (1999), Liquid retention and interfacial area in variably saturated porous media: Upscaling from single-pore to sample-scale model, *Water Resour. Res., 35*, 3591-3605.

Ransohoff, T. C., and C. J. Radke (1988), Laminar flow of a wetting liquid along corners of a predominantly gas-occupied noncircular pore, *J. Colloid Interface Sci., 121*, 392-401.

Raviv, U., P. Laurat, and J. Klein (2001), Fluidity of water confined to subnanometre films, *Nature, 413*, 51-54.

Read, A. D., and J. A. Kitchener (1969), Wetting films on silica, *J. Colloid Interface Sci., 30*, 391-398.

Rossi, C., and J. R. Nimmo (1994), Modeling of soil water retention from saturation to oven dryness, *Water Resour. Res., 30*, 701-708.

Schroth, M. H., S. J. Ahearn, J. S. Selker, and J. D. Istok (1996), Characterization of Miller-similar silica sands for laboratory hydrologic studies, *Soil Sci. Soc. Am. J., 60,* 1331-1339.

Silva, O., and J. Grifoll (2007), A soil-water retention function that includes the hyper-dry region through the BET adsorption isotherm, *Water Resour. Res., 43*, W11420, doi: 10.1029/2006WR005325.

Snyder, V. A. (1996), Statistical hydraulic conductivity models and scaling of capillary phenomena in porous media, *Soil Sci. Soc. Am. J., 60*, 771-774.

Suekane, T., S. Soukawa, S. Iwatani, S. Tsushima, and S. Hirai (2005), Behavior of supercritical CO_2 injected into porous media containing water, *Energy, 30*, 2370-2382.

Tokunaga, T. K., and J. Wan (1997), Water film flow along fracture surfaces of porous rock, *Water Resour. Res., 33*, 1287-1295.

Tokunaga, T. K., J. Wan, and S. R. Sutton (2001), Transient film flow on rough fracture surfaces, *Water Resour. Res., 36*, 1737-1746.

Tokunaga, T. K, K. R. Olson, and J. Wan (2004), Conditions necessary for capillary hysteresis in porous media: Tests of grain size and surface tension influences, *Water Resour. Res., 40*, W05111, doi:10.1029/2003WR002908.

Toledo, P. G., R. A. Novy, H. T. Davis, and L. E. Scriven (1990), Hydraulic conductivity of porous media at low water content, *Soil Sci. Soc. Am. J., 54*, 673-679.

Tuller, M., and D. Or (2002), Unsaturated hydraulic conductivity of structured porous media: A review of liquid configuration-based models, *Vadose Zone J., 1,* 14-37.

van Genuchten, M. Th. (1980), A closed form equation for predicting the hydraulic conductivity of unsaturated soils, *Soil Sci. Soc. Am. J., 44*, 892-898.

Waldron, L. J., J. L. McMurdie, and J. A. Vomocil (1961), Water retention by capillary forces in an ideal soil, *Soil Sci. Soc. Am. Proc., 25*, 265-267.

Wan, J., and T. K. Tokunaga (1997), Film straining of colloids in unsaturated porous media: Conceptual model and experimental testing, *Environ. Sci. Technol., 31*, 2413-2420.

Wei, C., and M. M. Dewoolkar (2006), Formulation of capillary hysteresis with internal state variables, Water Resour. Res., 42, W07405, doi:10.1029/2005WR004594.

Figures

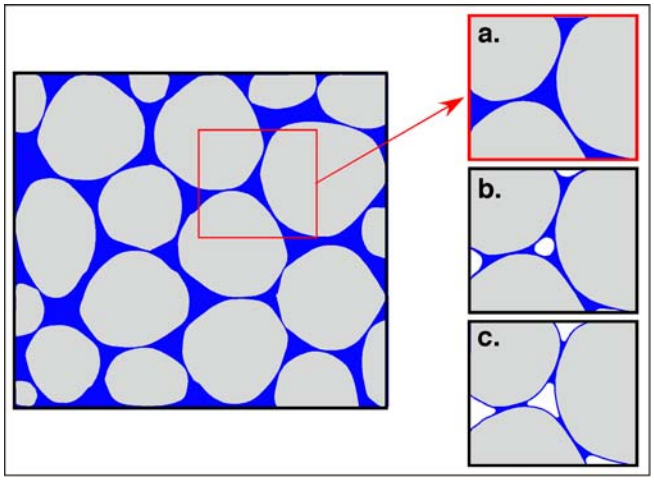

Figure 1. Categorization of saturation states for the wetting fluid. (**a.**) saturated, (**b.**) unsaturated, with interconnected pendular rings, and (**c.**) unsaturated with pendular rings separated by adsorbed liquid films.

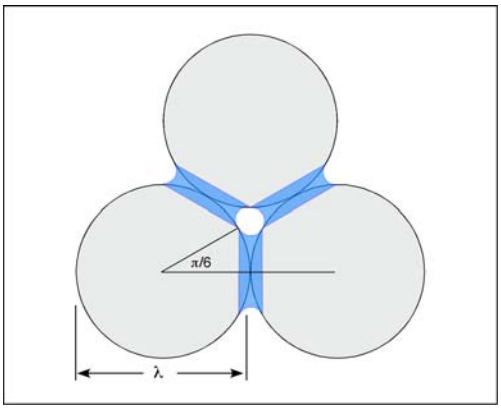

Figure 2. Configuration of pendular rings on three spherical grains. The scale-dependent critical matric potential and scale invariant critical saturation are associated with pendular ring perimeter at an angular radius = $\pi/6$.

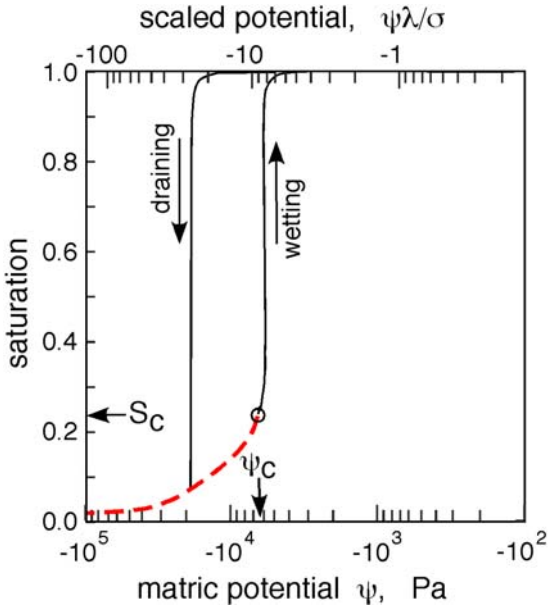

Figure 3. Illustrative moisture characteristic for a close pack of 0.1 mm diameter grains (surface tension = 7.27×10^{-2} N m^{-1}). The red dashed line indicates states where pendular rings are separated by thin films. ψ_c and S_c indicate the critical potential and critical saturation, respectively.

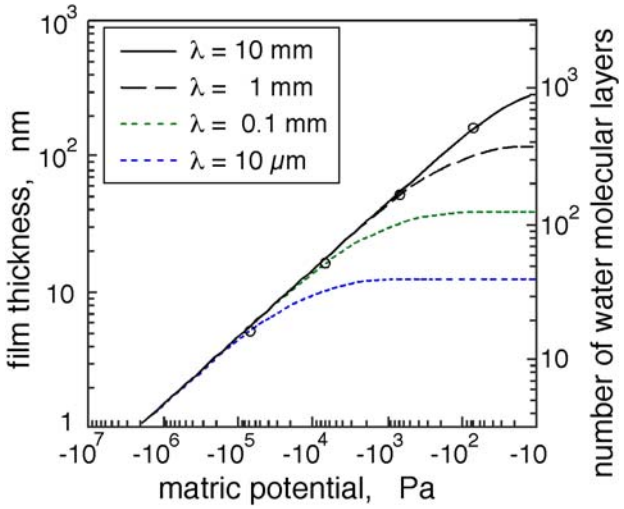

Figure 4. Dependence of film thicknesses on matric potential and grain size, for dilute, monovalent aqueous solutions. The open circles along each λ curve identify ψ_c values, below which pendular rings are disconnected.

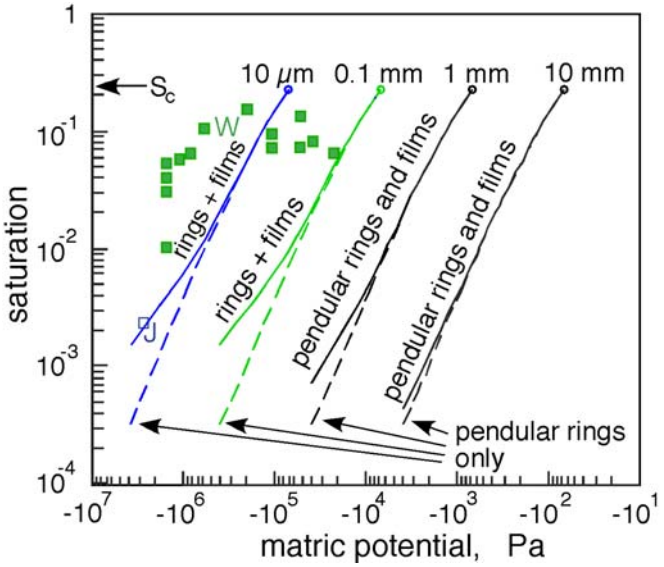

Figure 5. Calculated matric potential dependence of saturations for monodisperse set of water-wet, close pack spheres (10 μm, 0.1 mm, 1 mm, and 10 mm), at potentials ≤ ψ_c (ψ_c values are shown as open circles at highest energies for each grain size). Pendular ring contributions are shown as dashed lines. The sum of capillary rings and adsorbed films are shown as solid curves. Pendular ring connection/disconnection occurs at S_c = 0.243, indicated along the y-axis. Data from water drainage measurements on 99 μm glass spheres reported in *Waldron et al.* [1961] are indicated by the solid green squares within the "W" region (compare with calculations for 0.1 mm grains). Data from water vapor adsorption measurements on 10 to 15 μm glass spheres at the highest vapor pressures reported in *Jurinak et al.* [1962] are within the region indicated by the open blue square labeled "J", at ψ = -2.7 MPa (compare with calculations for 10 μm grains).

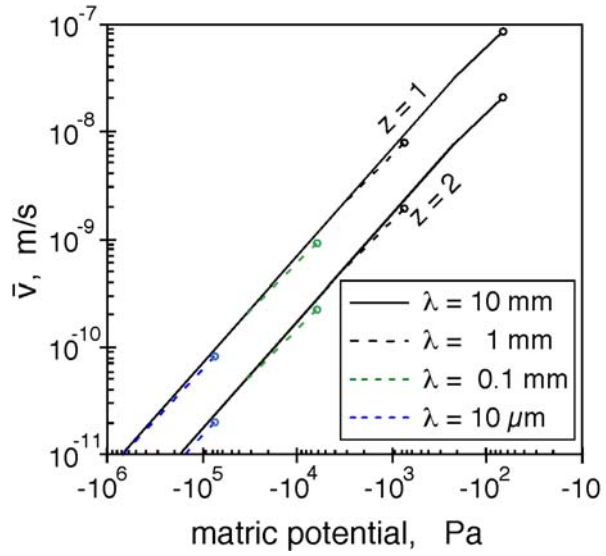

Figure 6. Dependence of average adsorbed film velocity on matric potential, grain size, and ionic charge, at low ionic strength and unit hydraulic head gradient.

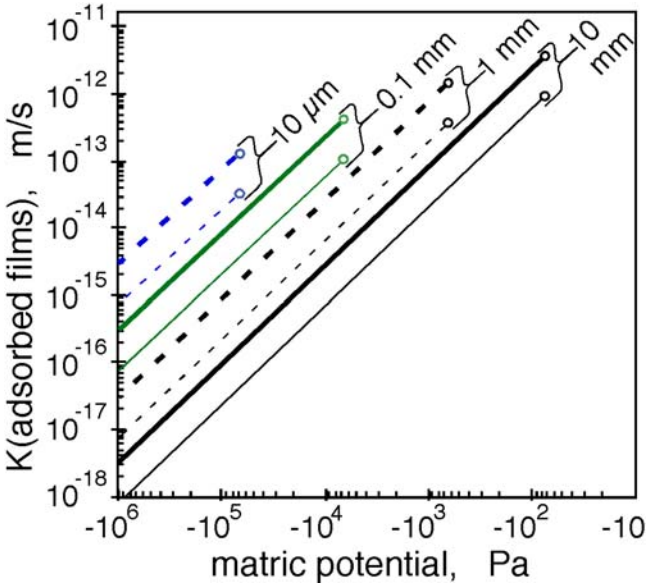

Figure 7. Predicted dependence of the unsaturated hydraulic conductivity on matric potential, grain size, and ion charge. Monovalent and divalent solutions are indicated by the thin and thick lines, respectively.